

High-temperature photomagnetism in Co-doped yttrium iron garnet films

A. B. Chizhik,* I. I. Davidenko,† A. Maziewski,‡ and A. Stupakiewicz
Institute of Physics, University of Białystok, 41 Lipowa, 15424 Białystok, Poland
 (Received 6 October 1997; revised manuscript received 27 February 1998)

Magnetization processes in $(\text{YCa})_3(\text{FeCoGe})_5\text{O}_{12}$ epitaxial films induced by linearly polarized argon laser light ($\lambda=0.488 \mu\text{m}$) were observed at room temperature. These processes happened through a displacement of boundary between magnetic domain phases with different in-plane magnetization components. The direction and amplitude of the displacement depended on the polarization direction and light intensity. The results are explained within the scope of a phenomenological theory of photoinduced anisotropy. The microscopic origin of the photomagnetic effect in investigated materials is qualitatively discussed. [S0163-1829(98)01822-0]

Peculiarities of energetic band structure, transport, and magnetic interactions in different materials cause the existence of photoinduced magnetic effects (PME's). Two types of PME are usually distinguished: light polarization independent and polarization sensitive.¹ The first ones include, e.g., changes of magnetic permeability and cubic magnetic anisotropy independent of light polarization. Photoinduced changes of uniaxial anisotropy, optical dichroism, and spin-reorientational effects appear in the polarization sensitive PME. PME's were investigated earlier in many kinds of magnetic materials: garnets, spinels, ferric borates, spin glasses, magnetite, and a wide class of ferrites.²⁻⁹ PME's have also been investigated in metals.^{10,11} Special intensive study was performed in garnets—ideal magnetic model materials due to their high quality and easy engineering of magnetic, electrical, and optical properties. Up to the present time PME was systematically investigated only at cryogenic temperatures.

It is well known, that light can affect magnetic properties for various reasons, which can by no means be reduced to the trivial heating of the crystal by the light. PME could be interpreted from the point of view of optical irradiation influence on electronic impurity subsystems in a crystal. As a consequence, exchange, and relativistic interactions can change. The most common condition of PME existence is the presence of highly anisotropic photosensitive ions in a crystal lattice, for example Fe^{2+} in YIG:Si or Co^{2+} in YIG:Co .^{1,12,13} This polarization dependence of the PME directly testifies to the fact that the relativistic PME mechanism is more probable in discussed materials. Therefore, neglecting changes of exchange interaction upon the effect of illumination, we consider that PME's are caused by the photoinduced changes of magnetic anisotropy.

In the present paper results of the investigation of polarization sensitive PME-photoinduced spin-reorientational effects in epitaxial films of Co-doped yttrium iron garnet are presented. Polarization sensitive PME was observed and studied at room temperature.

Our experimental studies were performed on about 10 μm -thick $\text{Y}_2\text{CaFe}_{3.9}\text{Co}_{0.1}\text{GeO}_{12}$ samples grown by liquid phase epitaxy on a (001) plane of a gadolinium gallium garnet substrate. Room-temperature magnetic properties of these samples were as follows:¹⁴ $4\pi M_S=90 \text{ G}$, constants of cubic and uniaxial magnetic anisotropy $K_1=-10^4 \text{ erg/cm}^3$

and $K_U=-2.5 \times 10^3 \text{ erg/cm}^3$. Easy magnetization axes are slightly inclined from the $\langle 111 \rangle$ -type directions. Magnetic domain phases with different in-plane magnetization components could be induced applying an external in-plane magnetic field.¹⁴ The scheme of the domain structure (DS) containing two phases (P_A and P_C) is shown in Fig. 1. The domain wall between phases (DWP's) is distinguished by the thick line. PME has been investigated only at liquid-nitrogen temperatures in these films.^{13,15}

Sample excitation was performed by an argon laser beam ($\lambda=0.488 \mu\text{m}$, $P=70 \text{ mW}$) focused on a film surface ($R=50 \mu\text{m}$) in a spatial region consisting of DWP's between mainly "black" and mainly "white" domain phases P_A and P_C [see the DS scheme in Fig. 1 and the DS image in Fig. 2(a)]. Any polarization direction of linearly polarized light φ measured from the [100] axis was available in the experiment. DS geometry and average magnetization changes were studied using the Faraday effect in two configurations of experimental setup. In the first configuration a magnetization

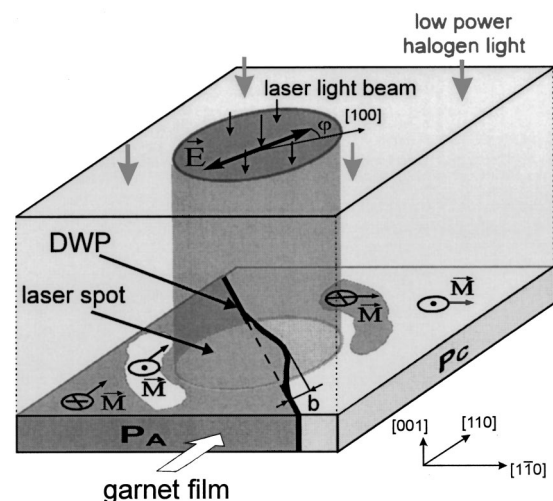


FIG. 1. Scheme of magnetic domain phases within the film region illuminated by both a low power halogen lamp and a linearly polarized laser beam. Typical notation for the description of magnetization orientation is used. Magnetization and in-plane components lie along the [110] and $[1\bar{1}0]$ directions in phases P_A and P_C , respectively. Dashed and thick lines show initial and final DWP states, respectively.

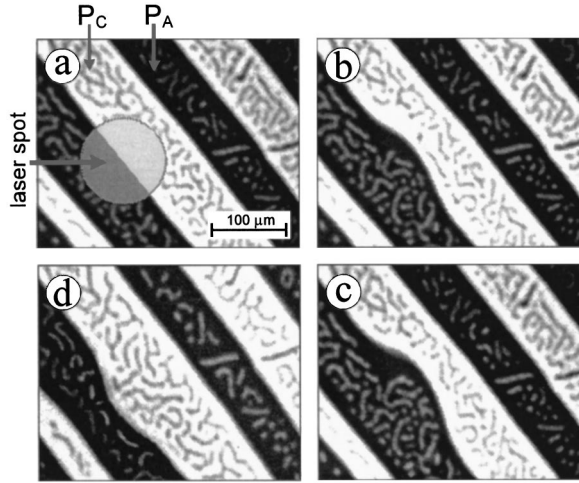


FIG. 2. Images of DS containing P_A and P_C phases: (a) before illumination; (b) and (d) after illumination with the linearly polarized light with polarization directions $\vec{E}||[1\bar{1}0]$ and $\vec{E}||[110]$, respectively, (c) after illumination with light with $\vec{E}||[110]$ in an external magnetic field 10 Oe along the $[110]$ direction. DS from (a) was initial for DS shown in (b,c). Initial DS for the structure registered in (d) was slightly different than DS in (a).

spatial distribution was investigated by an optical microscope with a low power halogen lamp. Domain structure images were registered by a sensitive charge-coupled device camera. A special spectral filter was used between the sample and the camera for the laser beam extinguishing to eliminate the laser distortion of domain structure image. Images were digitized by a frame grabber connected to an IBM PC and were specially digitally processed.¹⁴ In the second configuration only the argon laser beam was used for both the sample excitation and the magnetization process investigation. The process was studied using a standard polarized light modulation technique. The measured signal gave information about domains “black” and “white” areas in the laser illuminated spot.

Local photoinduced DWP displacement was observed within the illuminated film region [Figs. 2(b)–2(d)]. Direction and amplitude of the DWP bend depended on the light polarization state [see Figs. 2(b) and 2(d)]. The DWP position could also be changed by applying an in-plane magnetic field with a magnitude larger than the certain critical value of the starting field $H_S = (16.2 \pm 0.2)$ Oe connected with the sample coercivity. The DWP displacement amplitude measured without the illumination as a function of external magnetic field is presented in Fig. 3 by curve 1. The other two curves (2 and 3) in Fig. 3 describe the DWP displacement upon the simultaneous presence of the external magnetic field and illumination. The amplitude of the DWP displacement increases under the light power growth. Above a certain value of light power $P_S (\approx 0.2 \text{ W/cm}^2)$, changes in the domain phases happen even without an external magnetic field being applied. P_S is a fourfold symmetry function of the angle φ . It has minimums at $\varphi = \pi/4, 3\pi/4$ and goes to infinity at $\varphi = 0, \pi/2$. Formally, the polarized light influence on the DWP could be treated as an influence of an effective in-plane external magnetic field.

Light-induced DS transformations happen in a time scale extended to many seconds. It is shown in Fig. 4 where the

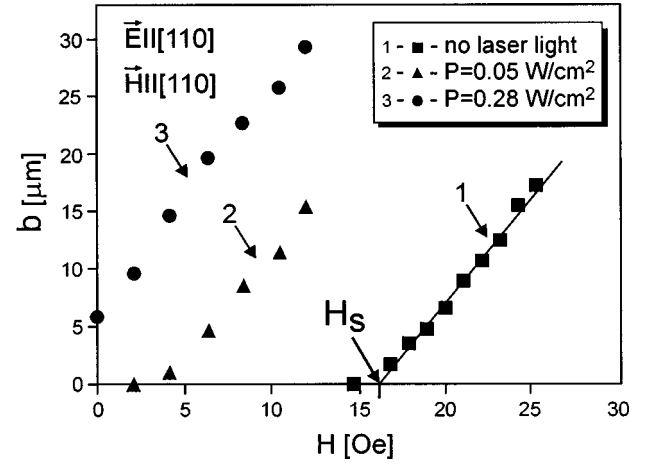


FIG. 3. Dependencies of the amplitude of the photoinduced DWP displacement on external magnetic field magnitude without illumination (curve 1) and with light illumination (curves 2 and 3) measured for different light intensities.

measured dynamics of the photoinduced DWP displacement is presented. The measured signal S arises only from the laser illuminated region. The signal is proportional to $(V_A - V_C)/(V_A + V_C)$, where V_A and V_C are the volumes of P_A and P_C magnetic phases, respectively. The photoinduced magnetization process starts with almost constant velocity $\nu(P, \varphi)$, then ν decreases and after a long enough time the signal reaches saturation. The final DS configuration and the final DWP displacement are presented in Figs. 2(b)–2(d) and Fig. 3, respectively. The final DWP displacement was measured for different orientations of light polarization with and without an external magnetic field being applied. The results are presented in Fig. 5. Amplitudes of these dependencies show a fourfold symmetry with maximums along the directions $[110]$ and $[1\bar{1}0]$. The light power used for exciting was not sufficient to overcome sample coercivity for the light polarization plane oriented near both the $[100]$ and $[010]$ directions without an external field being applied. The coercivity barrier could be decreased by applying a proper in-plane field. It could increase the sensitivity of the measurements of the photoinduced DWP displacement (see curve 2 in Fig. 5).

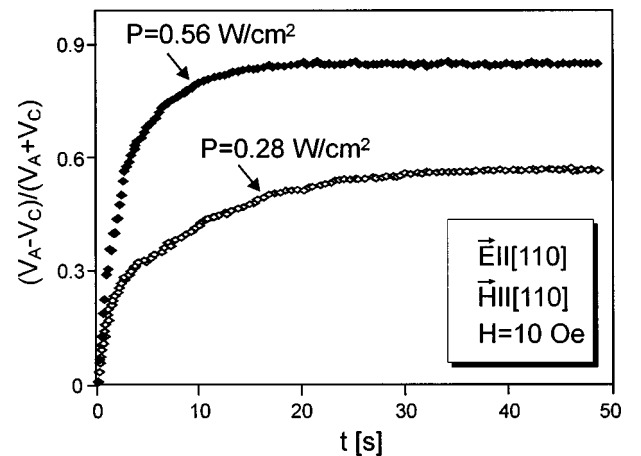


FIG. 4. Dynamics of photoinduced DWP displacement for different light intensities.

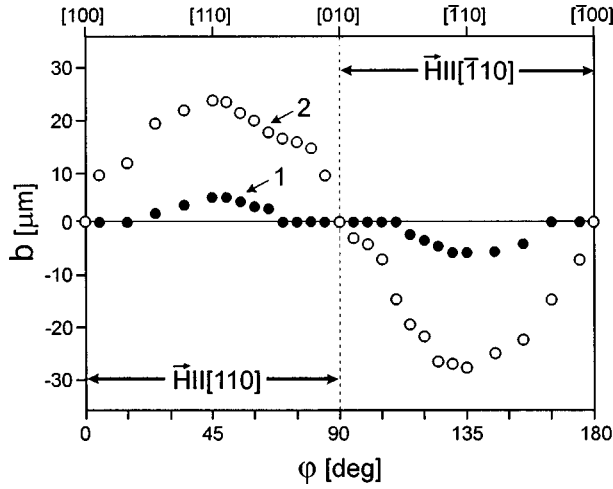


FIG. 5. Experimental dependencies of amplitude of photoinduced DWP displacement on the light polarization direction with external magnetic field (curve 1) and without external magnetic field (curve 2). An external field of 10.5 Oe was applied. The field was oriented along the $[110]$ and $[1\bar{1}0]$ directions for $\varphi \in \{0, \pi/2\}$, $\{\pi/2, \pi\}$, respectively.

The idea of photoinduced changes of the magnetic anisotropy could be used for a qualitative explanation of our experimental results. A simplified phenomenological model analogous to Refs. 15 and 16 was used. Within the scope of this model, energy of the magnetic anisotropy can be written in the following form:

$$\begin{aligned}
 W(\mathbf{m}, \mathbf{e}, t) = & -K_u m_z^2 + K_1 (m_x^2 m_y^2 + m_x^2 m_z^2 + m_y^2 m_z^2) + (1 \\
 & - \exp[-t/\tau]) [F_L (m_x m_y e_x e_y + m_x m_z e_x e_z \\
 & + m_y m_z e_y e_z) + G_L (m_x^2 e_x^2 + m_y^2 e_y^2 + m_z^2 e_z^2)],
 \end{aligned} \quad (1)$$

where K_u is the constant of the uniaxial anisotropy (growth and stress induced during the sample production), K_1 is the first constant of the cubic anisotropy, F_L and G_L characterize the photoinduced anisotropy arising from a linearly polarized light influence, e_i and m_i are the normalized components of the light polarization \mathbf{E} and the magnetization \mathbf{M} vectors, respectively, and τ is the characteristic time. Light-induced changes of both uniaxial and cubic anisotropy are neglected. The energetic term with G_L gives only a polarization-independent addition. In our calculations this term was not taken into account. Polarized light induces the following energy difference ΔW between domain phases P_A and P_C with different magnetization in-plane components:

$$\Delta W = 0.5 \sin^2 \Theta (1 - \exp[-t/\tau]) F_L \sin 2\varphi, \quad (2)$$

where Θ defines magnetization inclination from the $[001]$ direction. Formally, we can say that light induces the effective field H_L applied along the direction $[110]$. Transformed, Eq. (2) gives the expression for this field:

$$H_L = -\sin \Theta (1 - \exp[-t/\tau]) F_L \sin 2\varphi / (2M_S). \quad (3)$$

The obtained theoretical function $H_L(\varphi)$ qualitatively describes the experimentally observed angular symmetry of

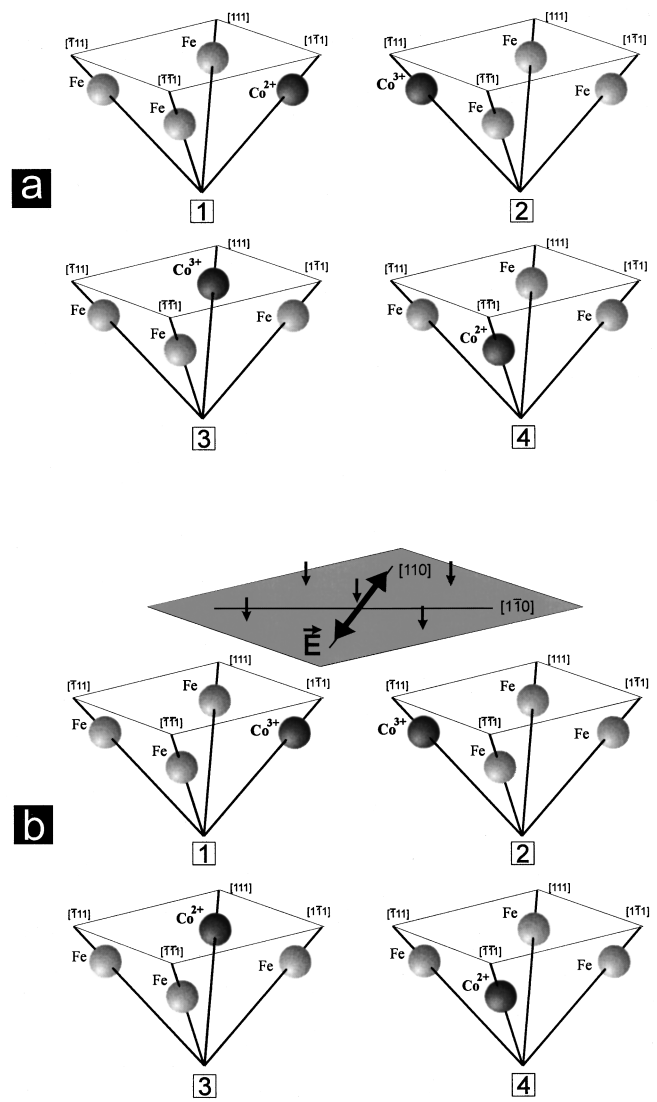


FIG. 6. Schematic representation of the light-induced changes of spatial Co^{2+} ions distribution. Configurations of four iron and cobalt ions in octahedral positions: (a) before light illumination (random cobalt ions distribution); (b) after polarized light excitation (one can find changes in the cobalt ion valence state in regions 1 and 3).

$b(\varphi)$. The different direction of the DWP displacement for opposite light polarization also follows from Eq. (3).

Tetrahedral and octahedral cobalt contributes to magnetic anisotropy. Usually isotropic cobalt distribution through tetrahedral positions contributes to cubic anisotropy, which could be deduced from comparison of the measured first cubic anisotropy constant K_1 and cobalt and iron ions single-ion contributions into K_1 .¹⁷ From the symmetry of the photoinduced anisotropy energy formed upon the illumination with linearly polarized light, one could try to determine the microscopic origin of the observed effects. Maximums of angular dependencies of the photoinduced DWP displacement $b(\varphi)$ (see Fig. 5) appear for the light polarization direction corresponding to the largest probability of excitation of photoactive centers occupying the octahedral sites. These sites are occupied by the strongly anisotropic magnetic ions Co^{2+} and, formally, Fe^{2+} . Comparing the energy levels of Co^{2+} and Fe^{2+} ions, one can conclude that at room tempera-

ture Co^{2+} is more stable than the Fe^{2+} state, i.e., octahedral Co^{2+} ions are responsible for observed photomagnetism.¹⁷ Therefore, it can be considered that one of the most probable reasons of PME existence in YIG:Co is the Co^{2+} presence in four types of octahedral sites and their redistribution under the linearly polarized light influence.

For an interpretation of the phenomenological formula given in Eq. (3), one can use Slonczewski's model¹⁸ with a single-ion contribution to the magnetic anisotropy. Let us consider strongly anisotropic Co^{2+} ions in octahedral positions for this purpose. Without light, four equivalent positions are distinguished. Two energetically nonequivalent octahedral positions appear in a sample excited by linearly polarized light with, e.g., $\mathbf{E} \parallel [110]$. It causes a spatial redistribution of Co^{2+} and Co^{3+} ions, see Fig. 6. A difference Δc of Co^{2+} ion concentration between these nonequivalent positions produces magnetic anisotropy described by the light induced anisotropy field given by Eq. (3). We have obtained $\Delta c \approx 10^{15}$ octahedral Co^{2+} per cm^3 using typical parameters for Co^{2+} ions¹⁷ as well as the results of the experimental estimation of H_L . This value is naturally much smaller than the total cobalt concentration in our film $c_{\text{tot}} \approx 10^{21}$ cobalt ions per cm^3 . In view of our experimental results we could propose the qualitative explanation of the PME physical nature in YIG:Co films at high temperatures.

The Co^{2+} ion has a stable valence in the garnet matrix because its energetic $3d$ levels do not coincide with energetic $3d$ levels of neighboring iron ions and weakly resonate with them. This is the reason for their considerable contribution into the energies of magnetic anisotropy and magnetostriction in cobalt-doped garnets. Hence, in studied material polarization, sensitive PME's are caused by the redistribution of populations of anisotropic photoactive centers in octahedral sites of a garnet crystal lattice occupied by Co^{2+} ions. The energetic level of Co^{2+} in an octahedral position lies roughly about 1 eV below that of Fe^{2+} [within a prohibited band, making up 2.9 eV (Ref. 17)], i.e., the energy consumption is necessary for thermoactivated electron transi-

tions, which means that the electron transitions could be caused only by a light quantum and the direct thermal excitation is improbable within the investigated temperature range. This circumstance creates obstacles to free the thermoactivated electron exit from the Co^{2+} ion and its motion between anisotropic photoactive centers through the conductive band. That makes the thermal relaxation of photoinduced nonequilibrium distribution of the site occupancies more difficult and makes the light influence on the magnetic system more effective at a higher temperature than in classical photomagnetic materials YIG:Si or YIG:Ge. Effectivity of the discussed PME is also high due to drastic changes of the magnetic anisotropy after the charge transfer between Co^{2+} and Co^{3+} ions in octahedral positions (a much smaller effect could be expected after the charge transfer between cobalt ions in the tetrahedral position.¹⁷)

Thus, we have demonstrated the existence of the polarization sensitive photomagnetic effect (light-induced magnetization process) in YIG:Co epitaxial films at room temperature. At lower temperatures the strength of the photomagnetic effect is higher than at room temperature.¹⁹ The obtained results are described within the scope of phenomenological theory based on the supposition about the light-induced anisotropy appearance within the illuminated region. The microscopic nature of the observed effect is also qualitatively discussed. Similar high-temperature photomagnetic effects can be expected in a wider class of magnetic semiconductors. The materials studied seem to be interesting because of both general knowledge and possible applications. The proposed method of a photomagnetic effect investigation based on domain structure analysis under the presence of external magnetic field for coercivity compensation is especially sensitive, as compared with traditional methods such as torque anisometry, ferromagnetic resonance study, etc. This method could be a powerful tool for the future study of photomagnetism.

This work was partially supported by Polish Grant No. 2P03B 061 14.

*Permanent address: Institute for Low Temperature Physics & Engineering, 47 Lenin Avenue, 310164 Kharkov, Ukraine.

†Permanent address: Interfaculty Research Laboratory of Information Recording Applied Problems, Kiev University, 60 Vladimirska, 252033 Kiev, Ukraine.

‡Author to whom correspondence should be addressed.

¹V. F. Kovalenko and E. L. Nagaev, *Sov. Phys. Usp.* **29**, 297 (1986); E. L. Nagaev, *Phys. Status Solidi B* **145**, 11 (1988), and references therein.

²R. W. Teale and P. W. Temple, *Phys. Rev. Lett.* **19**, 904 (1967).

³M. Pardavi-Horvath, P. E. Wigen, and G. Vértesy, *J. Appl. Phys.* **63**, 3110 (1988).

⁴S. N. Lyakhimets and K. Hisatake (unpublished)

⁵V. G. Veselago *et al.*, *Zh. Eksp. Teor. Fiz.* **97**, 559 (1990) [*JETP* **70**, 311 (1990)].

⁶G. S. Patrín, D. A. Velikanov, and G. A. Petrakovskii, *Zh. Eksp. Teor. Fiz.* **103**, 234 (1993) [*JETP* **76**, 128 (1993)].

⁷M. Ayadi and J. Ferre, *Phys. Rev. Lett.* **50**, 274 (1983).

⁸E. Katsnelson, *J. Appl. Phys.* **77**, 4604 (1995).

⁹I. Matsubara, K. Hisatake, K. Maeda, Y. Kawai, and K. Uematsu,

J. Magn. Magn. Mater. **104-107**, 427 (1992).

¹⁰V. L. Gurevich, R. Laiho, and A. V. Lashkul, *Phys. Rev. Lett.* **69**, 180 (1992).

¹¹V. V. Afonin, V. L. Gurevich, and R. Laiho, *Phys. Rev. B* **52**, 2090 (1995).

¹²F. K. Lotgering, *Phys. Chem. Solids* **36**, 1183 (1975).

¹³S. G. Rudov, M. V. Verchenko, V. G. Veselago, A. Maziewski, M. Tekielak, S. N. Lyakhimets, and J. M. Desvignes, *IEEE Trans. Magn.* **30**, 791 (1994).

¹⁴A. Maziewski, *J. Magn. Magn. Mater.* **88**, 325 (1990).

¹⁵A. B. Chizhik, S. N. Lyakhimets, A. Maziewski, and M. Tekielak, *J. Magn. Magn. Mater.* **140-144**, 2111 (1995).

¹⁶I. I. Davidenko, S. N. Lyakhimets, and V. F. Kovalenko, *Phase Transit.* **50**, 255 (1994).

¹⁷P. Hansen, K. Enke, and G. Winkler, in *Numerical Data and Functional Relationships in Science and Technology*, edited by K.-H. Hellwege and A. M. Hellwege, Landolt-Börnstein, New Series, Group III, Vol. 12, Pt. a (Springer-Verlag, Berlin, 1978).

¹⁸J. C. Slonczewski, *Phys. Rev.* **110**, 1341 (1958).

¹⁹The results of low-temperature study will be published elsewhere.